# Cyclic Voltammetric Behavior and Some Surface Characteristics of the Lead Electrode in Aqueous NaI Solutions

A. Mohamed Abd El-Halim,* Mohamed Hossam Fawzy,
Sayed Sabet Abd El Rehim, and Abd El Kader Saty
Department of Chemistry, Faculty of Science, Ain Shams University, Abbassia, Cairo, Egypt

(Received June 19, 1991)

Cyclic voltammograms of the quiescent lead electrode were examined in NaI solutions of various concentrations ranging between 0.03 and 1.30 M (1 M=1 mol dm$^{-3}$). Neither visual $PbI_2$ surface layer nor a typical voltammogram could be obtained unless five complete cycles were preformed in advance. This behavior was not observed for the cyclic voltammetric behavior of the lead electrode in chloride and bromide solutions and consequently could be referred to the less aggressive nature of the $I^-$ ion in comparison to the former halide ions. The data proved that the formation of a passivating layer of $PbI_2$ is a reversible process and depends primarily upon the concentration of NaI. By controlling the voltammetric conditions, particularly the number and mode of repeated cycles, thickening of the $PbI_2$ surface layer could be feasible. Moreover, the microstructure of the $PbI_2$ surface layer, as revealed by scanning electron microscopy, exhibited a simple correlation to the operating conditions. The obtained results pointed to the importance of the preceding complete cycles in building up of a relatively thick layer of spongy lead. Consequently, this layer is much more available for the formation of a thick, fine grained, and more compact $PbI_2$ surface layer by a reasonable number of only anodic spans. Investigation of the anodic surface products by X-ray diffractometry proved that the layers are formed of $PbI_2$ in the hexagonal crystalline structure and contamination by any other species could not be detected.

The electrochemical characteristics of the lead electrode in $H_2SO_4$ solution[1,2] and in HCl as well as NaCl solutions[3-5] have been intensively studied. The current interest in such studies refers to the importance of the $Pb/PbSO_4$ electrode in the storage lead acid battery and to the possibility of using the $Pb/PbCl_2$ electrode as an economical substitute for the Ag/AgCl electrode in sea water activated batteries.[6,7] In contrast the anodic behavior of lead in some other corrosive media such as bromide and iodide solutions, has not received adequate attention and very few literature has been published in this respect.[8]

Therefore, the present paper is devoted to investigate in details the cyclic voltammetric behavior of the lead electrode in NaI solutions and examination of the produced $PbI_2$ surface layer. In fact, this study was undertaken to achieve the following two purposes. Firstly to integrate our studies on the behavior of the lead electrode in HCl[9] and in $H_2SO_4$[10] solutions. Secondly, to provide some original data concerning preparation of the $Pb/PbI_2$ electrode by electrochemical means. This latter data may be helpful in development of a $PbI_2$–Mg accumulator analogous to the well established CuI–Mg accumulator.[11,12]

## Experimental

The working electrode was a lead rod of purity 99.999% (Johnson-Matthey and Co., Ltd.) prepared in the form of the so called protected electrode so that only its cross sectional area (1 cm$^2$) was in contact with the electrolyte. A platinum wire made of the purest metal was used as the counter electrode. The reference electrode was a saturated calomel electrode (SCE) prepared from very pure BDH chemicals.

The electrolytic cell consisted of a tall beaker containing the test electrolyte, the working electrode and the counter electrode. The counter electrode was fitted into a compartment separated from the main electrolyte by means of a $G_4$ sintered glass disc to affect separation of the anodic and cathodic reaction products. All potentials quoted in this paper were measured relative to the SCE using a salt bridge which was filled with the solution under investigation and placed with its tip almost touching the working electrode. In each experiment, a freshly prepared solution as well as a new set of electrodes were used. All experiments were performed at room temperature (25±2 °C).

The linear sweep voltammograms were determined with a Wenking Potentioscan model POS 73 and recorded automatically by means of an Ominographic $x$–$y$ recorder model 2000 . The cyclic voltammograms were obtained by sweeping the electrode potential linearly from the starting potential ($E_s$) to the switching potential ($E_\lambda$) and then reversing the sweep with the same rate up to $E_s$ in order to form one complete cycle. This process may be repeated several times without withdrawing the electrode from the electrolyte to examine the influence of the number of repeated cycles ($n$) on the characteristics of the cyclic voltammograms and the formed $PbI_2$ layer.

The morphology of the formed $PbI_2$ surface layer was examined with a scanning electron microscope (JEOL model JSM 35 ). X-Ray diffraction studies were carried out using a Philips X-ray diffractometer PW 1390, with a nickel filter and copper radiation.

## Results and Discussion

### 1. Cyclic Voltammetry

**1.1. Effect of NaI Concentration.** Cyclic voltammograms of the quiescent lead electrode were performed in NaI solutions of various concentrations (0.03—1.30 M ) at a sweep rate of 10 mV s$^{-1}$. The scan of the electrode potential was begun at $E_s$=$-$1000 mV and extended to $E_\lambda$=500 mV where the potential was reversed with the same rate to form a complete cycle. The process of cycling was repeated five times in each NaI solution and the last anodic half-cycle was recorded;

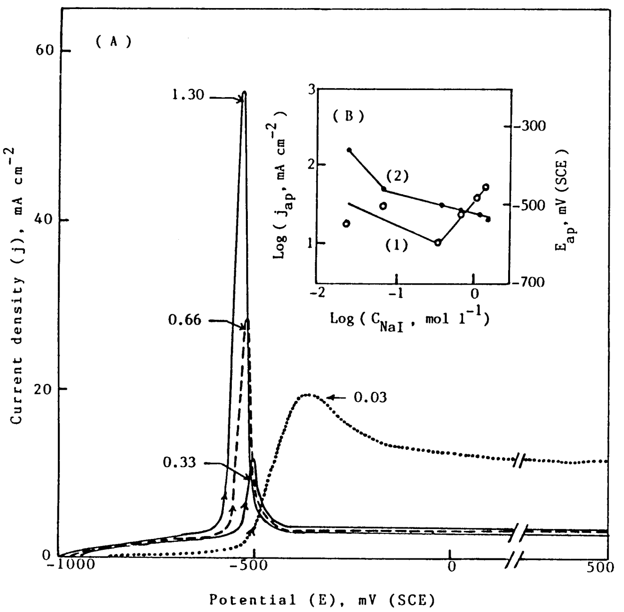

Fig. 1. (A) Effect of the concentration of NaI solution (0.03—1.30 M) on the voltammograms of the lead electrode at $\nu=10\ \mathrm{mV\,s^{-1}}$.
(B) The relation between $\log C_{\mathrm{NaI}}$ and each of: $\log j_{\mathrm{ap}}$ (line 1) and $E_{\mathrm{ap}}$ (line 2).

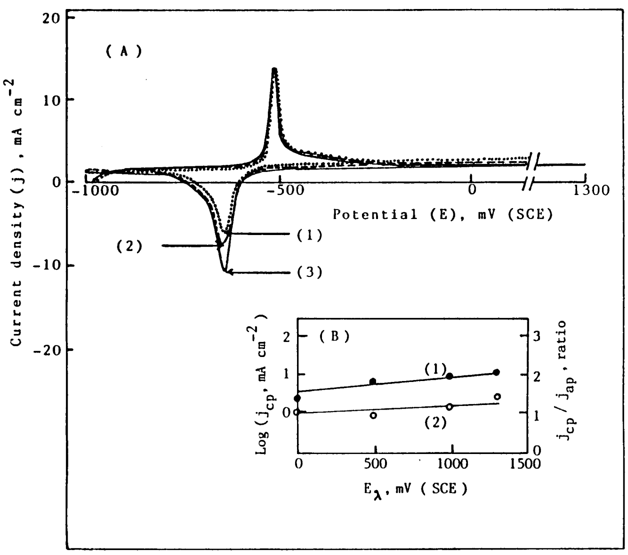

Fig. 2. (A) Effect of the potential scanning range on the cyclic voltammograms of the lead electrode in 0.33 M NaI solution: (1) $E_\lambda=500$, (2) $E_\lambda=1000$, and (3) $E_\lambda=1300$ mV.
(B) The relation between $E_\lambda$ and each of: $\log j_{\mathrm{cp}}$ (line 1) and the ratio $j_{\mathrm{cp}}/j_{\mathrm{ap}}$ (line 2).

Fig. 1 (A) includes some representative results. This procedure has been followed in order to detect clear and regular voltammograms and also to avoid the disturbance appeared in the primary four cycles. Such disturbance could be referred to the less aggressive nature of the $I^-$ ion in comparison to $Cl^-$ and $Br^-$ ions,[13] as would be expected from the standard potentials of the corresponding reactions:[14]

$$Pb+2\,Cl^- \longrightarrow PbCl_2+2e;\ E^\circ=268\ \mathrm{mV} \qquad (1)$$

$$Pb+2\,Br^- \longrightarrow PbBr_2+2e;\ E^\circ=280\ \mathrm{mV} \qquad (2)$$

$$Pb+2\,I^- \longrightarrow PbI_2+2e;\ E^\circ=365\ \mathrm{mV} \qquad (3)$$

Inspection of Fig. 1 (A) reveals that when the scan reaches the corrosion potential of lead, an anodic current starts to flow according to the reaction:

$$Pb \longrightarrow Pb^{2+}+2e;\ E^\circ=126\ \mathrm{mV} \qquad (4)$$

After attaining the so-called anodic peak current density ($j_{\mathrm{ap}}$), a sharp fall of the anodic current takes place ($C_{\mathrm{NaI}} \geqslant 0.33$ M). This is followed by a passive region extending over a wide range of potential in which a relatively low residual current ($j_r$) could be detected. This behavior could be due to the formation of a thin layer of $PbI_2$ (solubility product$=8.3\times10^{-9}$) by supersaturation of the solution near the electrode following the equation:

$$Pb^{2+}+2\,I^- \longrightarrow PbI_2 \qquad (5)$$

Figure 1 (A) depicts a gradual increase of $j_{\mathrm{ap}}$ with increase of $C_{\mathrm{NaI}}$ all over the range 0.33—1.30 M. This could also be represented by a linear relationship between logarithm $j_{\mathrm{ap}}$ and logarithm $C_{\mathrm{NaI}}$ (Fig. 1 (B)-line 1). In the light of these data it can be concluded that an increase of $C_{\mathrm{NaI}}$ accelerates reaction (3) leading to a corresponding increase of $j_{\mathrm{ap}}$ beside enhancing the building up of a passivating $PbI_2$ surface layer. A complementary explanation of the observed increase of $j_{\mathrm{ap}}$ with an increase of $C_{\mathrm{NaI}}$ may be correlated to the partial dissolution of the $PbI_2$ layer and formation of soluble complex ions in accordance with the equation:

$$PbI_2+I^- \longrightarrow [PbI_3]^- \qquad (6)$$

Such a complex is charaterized by an instability constant $3.6\times10^{-6}$.[14]

On the other hand in dilute (<0.33 M) NaI solutions $j_{\mathrm{ap}}$ increases again and show irregular dependence on $C_{\mathrm{NaI}}$. This feature is accompanied by incomplete passivation of the anode as could be detected from the passage of a considerably higher $j_r$ in the passive region (e.g. Fig. 1 (A)-the dotted curve). The observed change may be due to the subsequent decrease in the rate of diffusion of $I^-$ ions and hence the incomplete formation of a passivating $PbI_2$ surface layer.

A feature worthy of attention is that as $C_{\mathrm{NaI}}$ decreases, the potential ($E_{\mathrm{ap}}$) corresponding to $j_{\mathrm{ap}}$ shifts to less negative values (Fig. 1 (A)). Moreover, a plot of $E_{\mathrm{ap}}$ versus logarithm $C_{\mathrm{NaI}}$ gives a linear relationship which changes its slope at relatively low $C_{\mathrm{NaI}}$ values (Fig. 1 (B)-line 2 ). These results support the above discussion and indicate that as $C_{\mathrm{NaI}}$ increases, the passivating $PbI_2$ surface layer is formed more readily.

**1.2. Effect of the Potential Scanning Range.** Cyclic voltammograms of the quiescent lead electrode were recorded in 0.33 M NaI solution at a sweep rate of 10 mV s$^{-1}$. The scan of the electrode potential was started at −1000 mV and reversed at different $E\lambda$ values ranging between 0 and 1300 mV. Some representative voltammograms are depicted in Fig. 2 (A) which show that the anodic half-cycle exhibits the same general features as mentioned above. It is worthy to mention that at $E\lambda \geqslant$ 500 mV a yellow layer of $PbI_2$ could be visually seen on the electrode surface and $I_2$ was sometimes liberated at the counter electrode. On the other hand, the cathodic half-cycle shows a cathodic peak current density ($j_{cp}$), corresponding to reduction of the $PbI_2$ surface layer formed during the anodic half-cycle. Furthermore, Fig. 2 (A) illustrates a very slight increase of $j_{cp}$ with increase of $E\lambda$ or how far beyond $j_{ap}$ the scan is allowed to proceed before reversal. This relation is represented in semilogarithm form in Fig. 2 (B)-line 1. Such a result could be referred to thickening of the $PbI_2$ surface layer in the passive region. Similar results have been reported for the voltammograms of lead in HCl and NaCl solutions.[4] In addition, the ratio $j_{cp}/j_{ap}$ shows a slight dependence on $E\lambda$ and remains almost close to unity (Fig. 2 (B)-line 2). Only when the anodic span extends well into the passive region ($E\lambda$=1300 mV) $j_{cp}/j_{ap}$ attains 1.25. However, this feature is a characteristic parameter of reversible processes.[15]

**1.3. Effect of the Potential Sweeping Rate.** Figure 3 (A) shows some of the cyclic voltammograms of the quiescent lead electrode in 0.66 M NaI solution at various sweep rates ($\nu$) between 0.83 and 16.67 mV s$^{-1}$. The span limits $E_s$ (−1000 mV) and $E\lambda$ (500 mV) were selected so as to allow better coverage of the electrode with a passivating $PbI_2$ surface layer even at high $\nu$ values. The obtained voltammograms exhibit the same features and show a gradual increase of both $j_{ap}$ and $j_{cp}$ with increase of $\nu$, whilst $j_r$ remains nearly the same. Nevertheless, the ratio $j_{cp}/j_{ap}$ remains almost close to unity and does not change with $\nu$ (Fig. 3 (B)-line 1) indicating reversibility of the formation/reduction of the $PbI_2$ surface layer.[15] In addition, Fig. 3 (B)-line 2 illustrates the dependence of $j_{ap}$ on $\nu^{1/2}$ which implies a linear relationship, extrapolated to the origin, especially at $\nu$ values $\leqslant$ 10 mV s$^{-1}$. Such a relation points that the formation of the passivating $PbI_2$ surface layer is controlled by diffusion of the $I^-$ ions to the anode surface.[16] However, similar results and conclusion were reported by Ambrose et al.[3] for the formation of $PbCl_2$ surface layer in chloride solutions.

Moreover, inspection of Fig. 3 (A) reveals that $E_{ap}$ is independent on $\nu$; whereas, the potential ($E_{cp}$) corresponding to $j_{cp}$ shifts in the more negative direction with increase of $\nu$. Consequently, the separation of peak potentials ($\Delta E_p = E_{ap} - E_{cp}$) increases slightly with $\nu$ and ranges between 110 and 140 mV. Regarding that $\Delta E_p$ is a diagnostic test for reversible processes and that it is

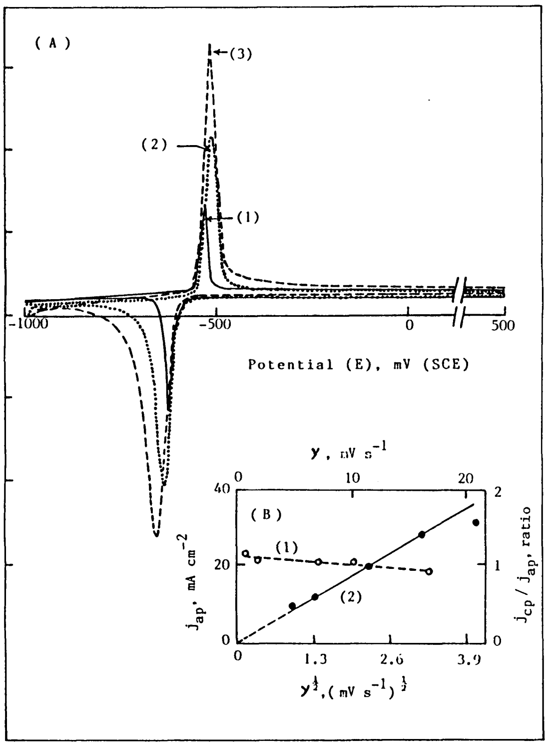

Fig. 3. (A) Effect of the potential sweeping rate ($\nu$) on the cyclic voltammograms of the lead electrode in 0.66 M NaI solution: (1) $\nu$=0.83, (2) $\nu$=5.00, and (3) $\nu$=16.67 mV s$^{-1}$.
(B) The relation between $\nu$ and the ratio $j_{cp}/j_{ap}$ (line 1) and the relation between $\nu^{1/2}$ and $j_{ap}$ (line 2).

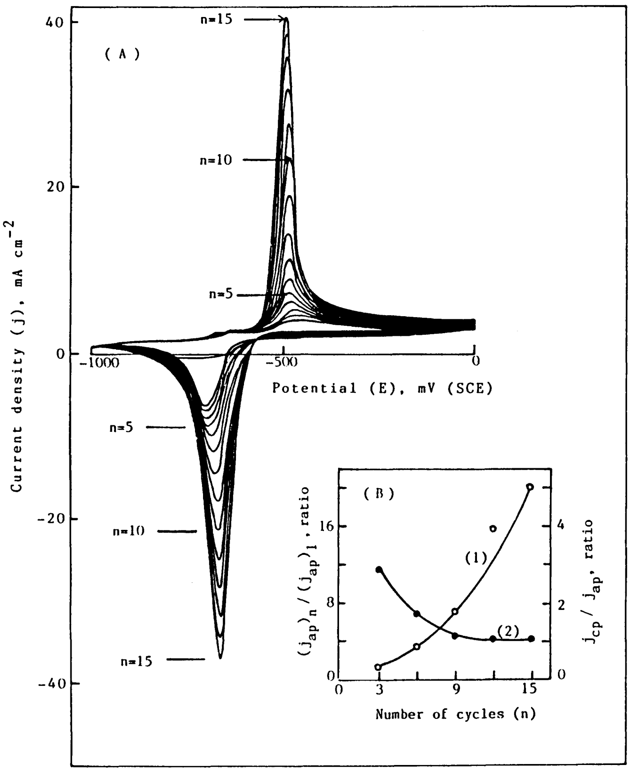

Fig. 4. (A) Effect of the number of repeated cycles ($n$=15 cycles) on the cyclic voltammograms of the lead electrode in 0.66 M NaI solution at $\nu$=50 mV s$^{-1}$.
(B) The relation between $n$ and each of: the ratio $(j_{cp})_n/(j_{ap})_1$ (line 1) and the ratio $j_{cp}/j_{ap}$ (line 2).

always close to 59/z mV at 25 °C.[17] The above results could be ascribed to the existence of uncompensated solution resistance ($R_u$) included in the measured potential; even when the tip of the reference electrode is designed for very close placement to the working electrode by use of a fine Luggin–Haber capillary tip. The practical effect of $R_u$, which increases with $\nu$, is to flatten the wave and shift $E_{cp}$ towards more negative potentials. Therefore an appreciable $R_u$ causes $\Delta E_p$ to be a function of $\nu$ even for a reversible electrode reaction.[17]

**1.4. Effect of the Number of Repeated Cycles.** Progressive cycling of the quiescent lead electrode between $E_s$=−1000 mV and $E\lambda$=0 mV was carried out in 0.66 M NaI solution at a sweep rate of 50 mV s$^{-1}$. Typical voltammograms are obtained, as can be seen in Fig. 4 (A), which imply a gradual increase of both $j_{ap}$ and $j_{cp}$ with the number of repeated cycles ($n$). This behavior may partially be ascribed to the fact that, on progressive cycling, the oxidation products formed during the anodic half-cycle are reduced during the consequent cathodic half-cycle. Accordingly it could be expected that the surface area of the lead electrode increases progressively with $n$ as a result of formation of spongy lead during the cathodic half-cycle.[10,18] Therefore, the increase of $j_{ap}$ measured during the following anodic half-cycle may be considered as a measure for the increase in the lead-free surface area on which the $PbI_2$ surface layer is likely to be formed.[9] Accordingly, the ratio of the anodic peak current density after $n$ cycles $(j_{ap})_n$ to that of the first cycle $(j_{ap})_1$ may be considered as a reasonable measure for thickening of the spongy lead, and hence the $PbI_2$ surface layer, by repeated cycling. The data of Fig. 4 (B)-line 1 depict such a relationship and this supports the above correlation. A supplementary interpretation of the successive increase of $j_{ap}$ and $j_{cp}$ with $n$ may be attributed to the liability of lead for oxidation by $I^-$ ions to form soluble complexes[15] according to the equation:

$$Pb+(2+x)I^- \longrightarrow [PbI_{2+x}]^{x-}+2e \qquad (7)$$

Furthermore, Fig. 4 (B)-line 2 shows that the ratio $j_{cp}/j_{ap}$ approaches 3 within the first few cycles and then decreases gradually with increase of $n$ until it reaches a steady value close to unity after 9 complete cycles. Such deviation of the ratio $j_{cp}/j_{ap}$ from unity has been previously ascribed to the further building up and thickening of the $PbI_2$ surface layer in the passive region. Moreover, previous investigators[4] pointed that reduction of some of the soluble complex species formed by reactions (6) and (7) may likely be a concurrent reaction beside reduction of the passivating layer. This suggestion may provide an additional explanation for the above-mentioned deviation.

**1.5. Effect of the Mode of Repeated Cycling.** Voltammograms of the quiescent lead electrode were traced under identical conditions of $E_s$ (−1000 mV), $E\lambda$ (0 mV), $\nu$ (50 mV s$^{-1}$), and $C_{NaI}$ (0.66 M). The following four sets of experiments were performed in order to investigate the influence of the mode of repeated cycling on the characteristics of the voltammograms.

set-1: 15 complete cycles
set-2: 5 complete cycles + 10 only anodic spans + 1 complete cycle.
set-3: 10 complete cycles + 5 only anodic spans + 1 complete cycle.

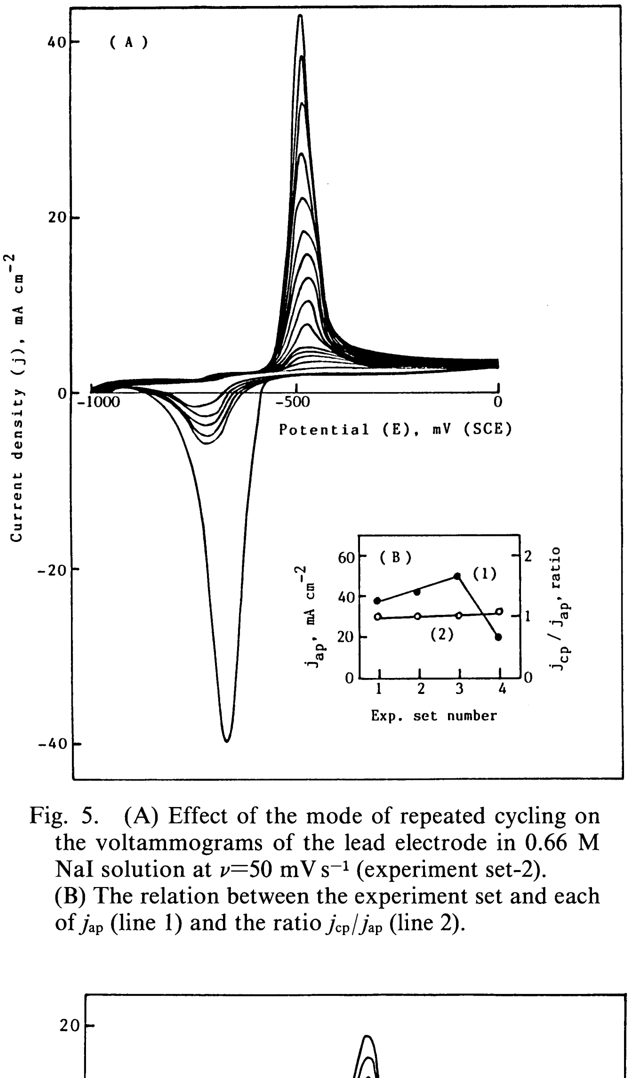

Fig. 5. (A) Effect of the mode of repeated cycling on the voltammograms of the lead electrode in 0.66 M NaI solution at $\nu$=50 mV s$^{-1}$ (experiment set-2).
(B) The relation between the experiment set and each of $j_{ap}$ (line 1) and the ratio $j_{cp}/j_{ap}$ (line 2).

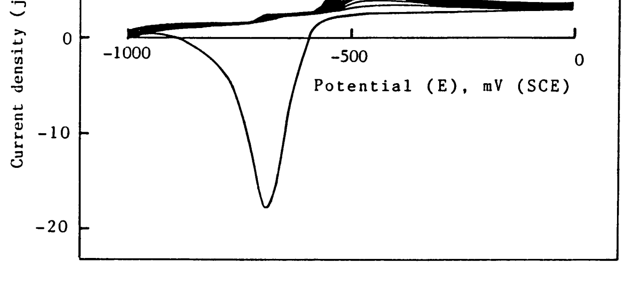

Fig. 6. Effect of the mode of repeated cycling on the voltammograms of the lead electrode in 0.66 M NaI solution at $\nu$=50 mV s$^{-1}$ (experiment set-4).

set-4: 15 only anodic spans
+ 1 complete cycle.

Some representative results are included in Figs. 4 (A), 5 (A), and 6. Inspection of the obtained voltammograms reveals that $j_{ap}$ of the final complete cycle, in the four sets, increases in the order: set-4<set-1<set-2set <3 respectively, Fig. 5 (B)-line 1. Accordingly, it would be expected that as the number of the initial complete cycles increases, in sets-2 and 3, a relatively thicker layer of spongy lead is formed. Moreover, the thickness of this layer is interrelated with the increase of $j_{ap}$ and hence with the readiness of formation of the $PbI_2$ by the consecutive only anodic spans, irrespective of their number. This point of view is supported by the experimental fact that $j_{ap}$ of the final complete cycle in set-4 is the least with respect to those observed in the other sets.

In addition, the ratio $j_{cp}/j_{ap}$ of the final complete cycle in each of the four sets of experiments is close to unity (Fig. 5 (B)-line 2 ). This implies the persisting reversibility of the electrode reaction in spite of the different modes of repeated cycling. In other words, this means that the whole $PbI_2$ formed during the only anodic spans, in sets-2 and 3, is reduced in the final cathodic half-cycle.

## 2. Surface Morphology.

**2.1. Effect of NaI Concentration.** The influence of $C_{NaI}$ within the range 0.07—1.30 M on the morphology of the $PbI_2$ surface layer formed by one anodic half-cycle on a fresh electrode was studied. The samples were prepared under identical conditions of $E_s$ (−1000 mV), $E\lambda$ (500 mV) and $\nu$ (10 mV s$^{-1}$). The electron micrographs in Fig. 7 show some representative results. At relatively low $C_{NaI}$ (0.33 M), the electrode is sparsely covered by few dihedral small crystals leaving some big non-covered areas (Fig. 7 (A)). This result agrees well with the experimental observation that neither the cyclic voltammogram nor the $PbI_2$ surface layer became clear and regular unless five complete cycles, at least, were performed in advance. This behavior may be due to the less aggressive nature of the $I^-$ ion with respect to the other halide ions.[13] Nevertheless. on increasing $C_{NaI}$ gradually both the nucleation density and the crystal growth increase to a higher extent giving rise to a better coverage of the electrode surface. Finally, when $C_{NaI}$ reaches 1.30 M, the electrode surface is nearly completely covered with larger irregularly shaped hexagonal crystals including some smaller dihedral grains between them (Fig. 7 (B)). These data are in accordance with the observed increase of $j_{ap}$ and shifting of $E_{ap}$ towards more negative values with increase of $C_{NaI}$.

**2.2. Effect of the Potential Scanning Range.** The morphology of the formed $PbI_2$ surface layers was examined as a function of $E\lambda$, ranging between 0 and 1300 mV, and some of the electron micrographs taken are shown in Fig. 8. The same operating conditions of $E_s$ (−1000 mV), $\nu$ (5 mV s$^{-1}$), $C_{NaI}$ (0.33 M), and $n$ (5 complete cycles followed by one anodic half-cycle) were utilized for preparation of all the examined samples. At $E\lambda$ values in the near passive region, e.g. 0−500 mV, the electrode surface is covered with a basal layer of fine grained crystals on which few larger dihedral excrescences could be observed, as represented by Fig. 8 (A). However, as $E\lambda$ increases there is a regular trend of increasing the coverage of the electrode surface with elongated dihedral grains oriented at random, such as

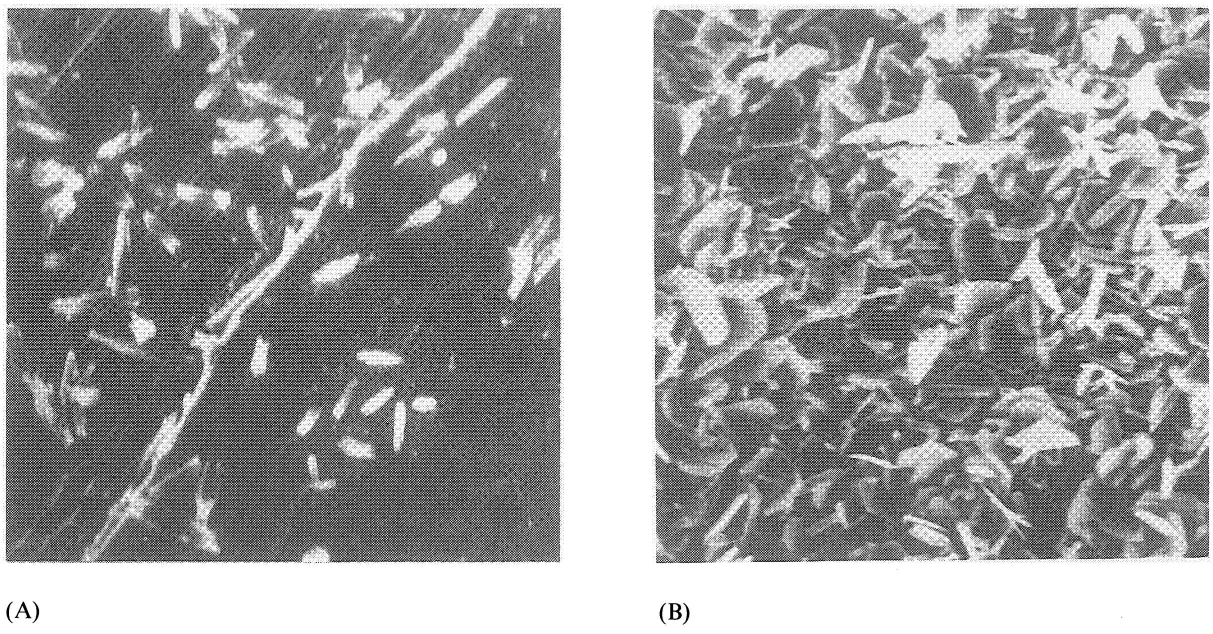
(A) (B)

Fig. 7. Electron micrographs of the formed $PbI_2$ surface layers at $\nu$=10 mV s$^{-1}$, $E_\lambda$=500 mV, and magnification 2000×.
(A) $C_{NaI}$=0.33 and (B) $C_{NaI}$=1.30 M.

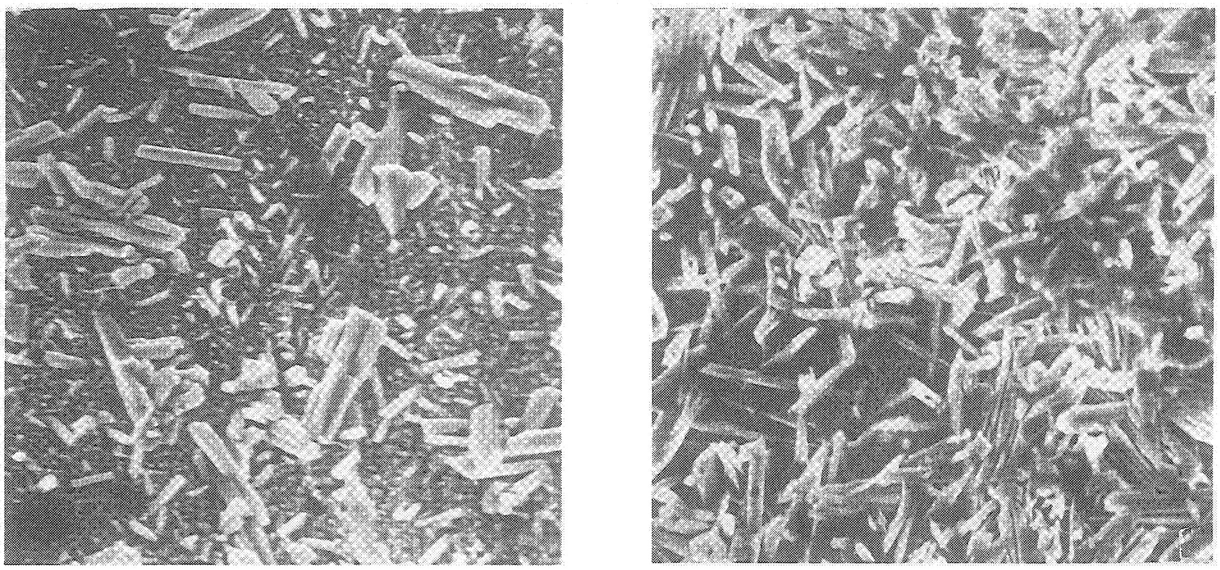

(A) (B)

Fig. 8. Electron niicrographs of the formed $PbI_2$ surface layers in 0.33 M NaI solution at $\nu$=5 mV $s^{-1}$ and magnification 2000×.
(A) $E_\lambda$=500 and (B) $E_\lambda$=1300 mV.

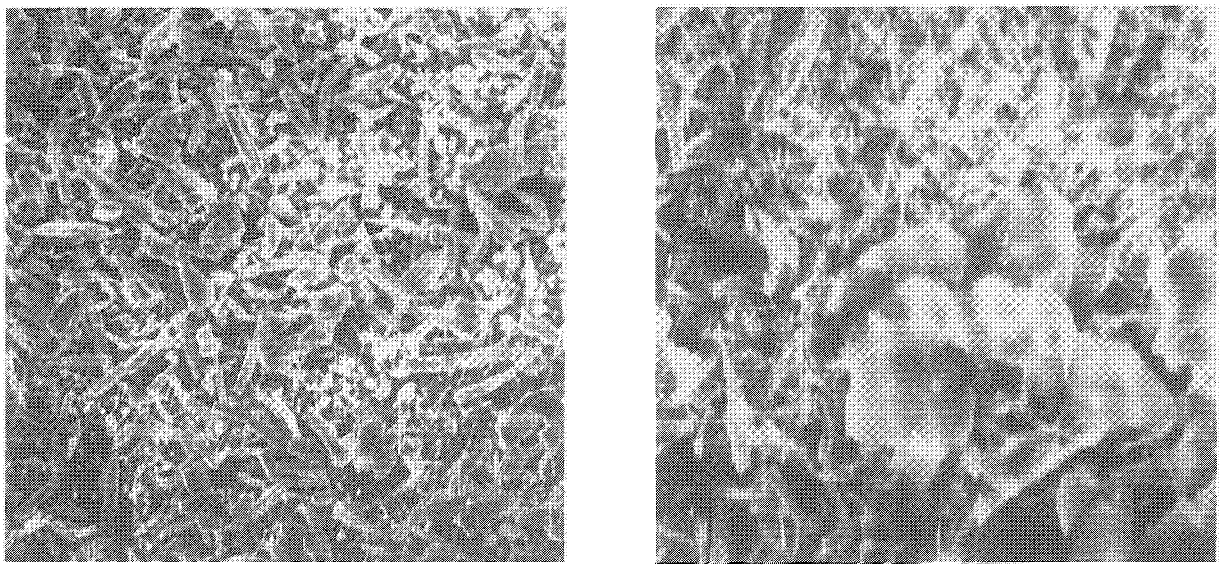

(A) (B)

Fig. 9. Electron micrographs of the formed $PbI_2$ surface layers in 0.66 M NaI solution at $E_\lambda$=500 mV and magnification 2000×.
(A) $\nu$=0.83 and (B) $\nu$=16.67 mV $s^{-1}$.

that shown in Fig. 8 (B). This morphological modification could be due to recrystallization and further thickening of the $PbI_2$ surface layer as indicated by the passage of $j_r$ in the passive region. Moreover, the obtained data agree with the observed increase of both $j_{cp}$ and the ratio $j_{cp}/j_{ap}$ with increase of $E\lambda$ (Fig. 2 (B)).

**2.3. Effect of the Potential Sweeping Rate.** The influence of $\nu$, ranging between 0.83 and 16.67 mV $s^{-1}$, on the microstructure of the formed $PbI_2$ surface layers was examined. The samples were prepared under the same conditions of $E_s$ (−1000 mV), $E\lambda$ (500 mV), $C_{NaI}$ (0.66 M), and $n$ (5 complete cycles followed by one anodic half-cycle). In general, at low $\nu$ values, a relatively thick layer of $PbI_2$ consists of close-packed small dihedral crystals almost having the same shape and size is formed as represented by Fig. 9 (A). Such a structure is characteristic for rapid or instantaneous nucleation process.[19)]

Thereafter, a gradual increase of $\nu$ leads to a corresponding change in the growth morphology depicted by grain refinement and thinning of the $PbI_2$ surface layer. Accordingly, Fig. 9 (B) shows the electron micrograph taken for the $PbI_2$ surface layer formed at the highest examined rate. The latter consists of a coherent accumulation of irregularly shaped small crystals that form a basal thin layer on which some bigger plate-like patches are formed. The growth of such patches could be referred to the slow, incomplete, passivation which allows continued supply of $Pb^{2+}$ ions until near beyond $E_{ap}$ and hence permits further growth of some of the initially formed $PbI_2$ crystals before complete passivation. This point of view is supported by the observed increase of both $j_{ap}$ and the width of $E_{ap}$ with increase of $\nu$ (Fig. 3).

**2.4. Effect of the Mode of Repeated Cycling.** $PbI_2$ surface layers were prepared under identical conditions of $E_s$ (−1000 mV), $E\lambda$ (0 mV), $\nu$ (50 mV s$^{-1}$), and $C_{NaI}$ (0.66 M). The following three sets of experiments were employed to examine the influence of the mode of repeated cycling on the morphology of the formed layers.

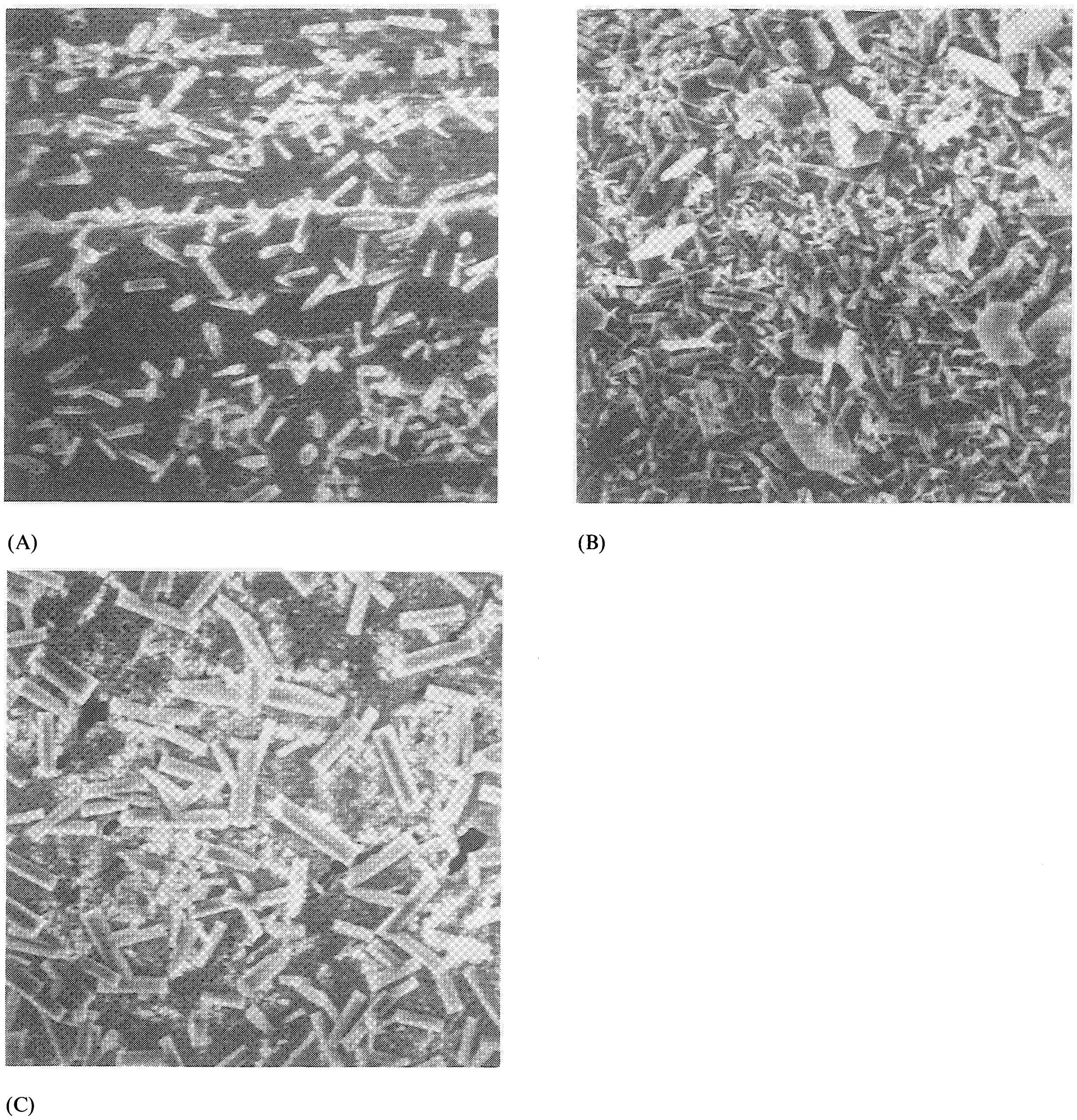
(A) (B) (C)

Fig. 10. Electron micrographs of the formed $PbI_2$ surface layers in 0.66 M NaI solution at $E_\lambda$=0 mV, $\nu$=50 mV s$^{-1}$ and magnification 2000×.
(A) Experiment set-5, (B) Experiment set-6, and (C) Experiment set-7.

Table 1. Characteristics of X-Ray Diffraction Patterns of the $PbI_2$ Formed at $\nu$=10 mV s$^{-1}$, $E_\lambda$=500 mV, and $n$=1 Complete Cycle Followed by 1 Anodic Half-Cycle. Sample I in 1.30 M, Sample II in 0.66 M, and Sample III in 0.33 M NaI Solutions

| Sample number | Observed | | *h k l* | Observed lattice parameters (Å)[a] | |
|---|---|---|---|---|---|
| | *d* (Å) | $I/I_0$ | | *a* | *c* |
| I | 6.979 | 33 | (001) | 4.547 | 6.979 |
| | 3.435 | 18 | (101) | | |
| | 2.599 | 76 | (102) | | |
| | 2.295 | 100 | (110) | | |
| II | 2.336 | 32 | (003) | 4.590 | 7.008 |
| | 2.025 | 36 | (103) | | |
| | 1.729 | 100 | (202) | | |
| III | 3.435 | 4 | (101) | 4.520 | 6.976 |
| | 2.341 | 80 | (003) | | |
| | 2.025 | 100 | (103) | | |
| | 1.732 | 18 | (004) | | |
| | 1.490 | 10 | (203) | | |

a) The standard lattice parameters are: $a$=4.557, and $c$=6.979 Å.

set-5: 15 complete cycles + 1 only anodic span.
set-6: 10 complete cycles + 5 only anodic spans.
set-7: 15 only anodic spans.

Inspection of Fig. 10 (A) reveals that the $PbI_2$ surface layer produced by the experiment set-5 is formed of small dihedral elongated crystals widely isolated from each other. This appearance implies a high nucleation density of $PbI_2$ which could be ascribed to the successive formation of spongy lead layer, of increased surface area, by the 15 repeated cycles.[10,18] Such a layer is more readily available for the formation of $PbI_2$ by a rapid nucleation process during the consequent one only-anodic span giving rise to a large number of small crystals of nearly the same shape and size.[19] This phenomenon is amplified in the $PbI_2$ surface layer formed by the experiment set-6 and it could be attributed to increase of the only anodic spans consecutive to the formation of a reasonable spongy lead surface layer. Accordingly, Fig. 10 (B) illustrates a thicker and finer grained $PbI_2$ surface layer which consists of smaller dihedral elongated crystals in the form of close-grained texture and covered by some distorted larger hexagonal crystals.

On the other hand, the experiment set-7 leads to the formation of a very thin fine grained basal layer sparsely covered by larger dihedral crystals (Fig. 10 (C)). A comparison between Figs. 10 (B) and (C) indicates the great importance of the role played by the preceding complete cycles in the building up of the $PbI_2$ surface layer by the consecutive only anodic spans.

### 3. X-Ray Diffractometry.

The influence of the operating variables $C_{NaI}$, $E_\lambda$, $\nu$, and $n$ on the X-ray diffraction patterns of the produced surface layers was examined. In general, the obtained data showed that all the layers are formed of $PbI_2$ in the crystalline hexagonal structure and are not contaminated by any other products. This conclusion could be confirmed by the observed congruence, to a great extent, between the calculated and the standard lattice parameters. The role played by any of the variables mentioned above is limited to a minor modification of the growth form as indicated by the corresponding changes in the (*h k l*) planes and/or the relative intensities ($I/I_0$) of the peaks. For example, Table 1 includes some representative results which show the effect of $C_{NaI}$ on the X-ray characteristics of the produced $PbI_2$ surface layers. The most noticeable feature is that a decrease of $C_{NaI}$ leads to appearance of some new crystal planes (*h k l*) and disappearance of others. Of course, this is also accompanied by variation of the most preferred orientation of the crystal planes.

### References

1) D. Pavlov, C. N. Poulieff, E. Klaja, and N. Lordanov, *J. Electrochem. Soc.*, **116**, 316 (1969).

2) G. Archdale and J. A. Harrison, *J. Electroanal. Chem.*, **43**, 321 (1973).

3) J. Ambrose, R. G. Barradas, K. Belinko, and D. W. Shoesmith, *J. Colloid Interface Sci.*, **47**, 441 (1974).

4) R. G. Barradas, K. Belinko, and J. Ambrose, *Can. J. Chem.*, **53**, 389 (1975).

5) R. G. Barradas and S. Fletcher, *Electrochim. Acta,* **22**, 237 (1977).

6) J. R. Coleman, Can. Patent 973607 (1975).

7) L. J. Burant, U. S. Patent 4021597 (1977).

8) G. W. D. Briggs and W. F. K. Wynne-Jones, *J. Chem. Soc.*, **1956**, 2966.

9) S. S. Abd El Rehim, A. M. Abd El-Halim, and E. E. Foad, *Surf. Technol.*, **18**, 313 (1983).

10 S. S. Abd El Rehim, A. M. Abd El-Halim, and E. E. Foad, *Surf. Technol.*, **21**, 161 (1984).

11) J. Root, U. S. Patent 3450570 (1969).

12) N. Margalit, *J. Electrochem. Soc.*, **122**, 1005 (1975).

13) S. S. Abd El Rehim, S. M. Abd El Wahaab, and E. A. Abd El Maguid, *Werkst. Korros.*, **37**, 550 (1986).

14) W. M. Latimer, "Oxidation Potentials," 2nd ed,

Prentice-Hall Inc., Englewood Cliff, N. J. (1964), p. 153.

15) D. T. Sawyer and J. L. Roberts, Jr., "Experimental Electrochemistry for Chemists," John Wiley & Sons, New York (1974), pp. 68, 338.

16) T. Berzins and P. Delahay, *J. Am. Chem. Soc.*, **75**, 555 (1953).

17) A. J. Bard and L. R. Faulkner, "Electrochemical Methods—Fundamentals and Applications," John Wiley & Sons, New York (1980), pp. 219—228.

18) F. Beck and H. Krohn, *J. Power Sources,* **12**, 9 (1984).

19) R. G. Barradas, K. Belinko, and W. Shoesmith, *Electrochim. Acta,* **21**, 357 (1976).